Structure and Properties of Thiolatorhodium Complexes, $Rh(SC_6H_4$-*p*-X$)(PMe_3)_3$ (X = Me, OMe)

Kohtaro Osakada,* Kouji Hataya, and Takakazu Yamamoto*

Research Laboratory of Resources Utilization, Tokyo Institute of Technology, 4259 Nagatsuta, Midori-ku, Yokohama 227, Japan

Received March 22, 1993

Summary: Reactions of $[Rh(PMe_3)_4]Cl$ with $NaSC_6H_4$-p-Me and with $NaSC_6H_4$-p-OMe give $Rh(SC_6H_4$-p-X$)(PMe_3)_3$ (1, X = Me; 2, X = OMe) whose structures were determined by X-ray crystallography. Complexes 1 and 2 react with HSC_6H_4-p-Me and HSC_6H_4-p-OMe, respectively, to give the corresponding cis,mer- and trans-,mer-$RhH(SC_6H_4$-p-X$)_2(PMe_3)_3$. Isomerization of the cis,mer product to the trans,mer isomer was observed during the reaction. cis,mer- and trans,mer-$RhH(SPh)_2(PMe_3)_3$ react with HSC_6H_4-p-OMe to undergo exchange of the thiolato ligand with the SC_6H_4-p-OMe group to give mixtures of trans,mer-$RhH(SAr)_2(PMe_3)_3$ (Ar = Ph or C_6H_4-p-OMe).

Thiolato complexes of group 8–10 metals have attracted increasing attention[1] since they are believed to play important roles in various synthetic organic reactions catalyzed by transition metal complexes.[2] On the other hand, there have been a limited number of reports on the reaction details of the thiolato complexes especially of the complexes having nonbridging thiolato ligands. Recently, we have prepared a rhodium phosphine complex with a nonbridging thiolato ligand, $Rh(SPh)(PMe_3)_3$, which underwent facile oxidative addition of the Si–H bond of a hydrosilane as well as of the C–H bond of phenylacetylene to give the corresponding Rh(III) complexes.[3] $Rh(SPh)(PMe_3)_3$ reacts also with HSPh to give *cis,mer*- and *trans,mer*-$RhH(SPh)_2(PMe_3)_2$ as the kinetic and thermodynamic products, respectively. Although the cis,mer product undergoes isomerization into the trans,mer isomer during the reaction, the detailed mechanism of the isomerization has not been fully elucidated. Here we report preparation, structures of analogous thiolatorhodium complexes $Rh(SC_6H_4$-*p*-X$)(PMe_3)_3$ (X = Me, OMe), and the reaction with thiols to discuss the pathway of the above isomerization of the *cis,mer*- to *trans,mer*-bis(thiolato)-hydridorhodium(III) complexes.

Results and Discussion

Preparation and Structures of $Rh(SC_6H_4$-*p*-X$)(PMe_3)_3$. Complex $[Rh(PMe_3)_4]Cl$ reacts with $NaSC_6H_4$-*p*-Me and with $NaSC_6H_4$-*p*-OMe to give the corresponding thiolato complexes $Rh(SC_6H_4$-*p*-X$)(PMe_3)_3$ (1, X = Me, and 2, X = OMe) as air-sensitive orange crystals. Com-

$$[Rh(PMe_3)_4]Cl + NaSC_6H_4\text{-}p\text{-}X \xrightarrow{-NaCl} Rh(SC_6H_4\text{-}p\text{-}X)(PMe_3)_3 + PMe_3$$
$$1,\ X = Me;\ 2,\ X = OMe$$

plexes 1 and 2 give satisfactory analytical and NMR data for the structure. Previously, we have reported that $[Rh(PMe_3)_4]Cl$ reacted with $NaSC_6H_4$-*p*-OMe to give dioxygen coordinated complex $Rh(SC_6H_4$-*p*-OMe$)(O_2)(PMe_3)_3$, probably through formation of 2 and its ensuing reaction with O_2 contained in the reaction system, and that the isolation of 2 was not feasible due to its extremely high sensitivity toward air.[3a] However, improvement of the reaction conditions in further study enabled the isolation of 2 in 38% yield. Complex 1 similarly isolated also reacts readily with oxygen to give $Rh(SC_6H_4$-*p*-Me$)(O_2)(PMe_3)_3$ (3) which shows satisfactory analytical and NMR data.

Figures 1 and 2 show the molecular structures of 1 and 2 determined by X-ray crystallography. The molecules have slightly distorted square-planar coordination around the rhodium center. The aromatic plane of 1 is almost perpendicular to the coordination plane, while that of 2 is declined from the coordination plane by ca. 35°. Table I summarizes selected bond distances and angles. The Rh–S bond distances slightly decrease in the order

(1) (a) Bianchini, C.; Mealli, C.; Meli, A.; Sabat, M. *Inorg. Chem.* **1986**, *25*, 4617. (b) Bianchini, C.; Meli, A.; Dapporto, P.; Tofanari, A.; Zanello, P. *Ibid.* **1987**, *26*, 3677. (c) Amarasekera, J.; Rauchfuss, T. B.; Wilson, S. R. *J. Chem. Soc., Chem. Commun.* **1989**, 14. (d) Amarasekera, J.; Rauchfuss, T. B. *Inorg. Chem.* **1989**, *28*, 3875. (e) Dev, S.; Imagawa, K.; Mizobe, Y.; Cheng, G.; Wakatsuki, Y.; Yamazaki, H.; Hidai, M. *Organometallics* **1989**, *8*, 1232. (f) Dev, S.; Mizobe, Y.; Hidai, M. *Inorg. Chem.* **1990**, *29*, 4797. (g) Matsuzaka, H.; Hirayama, Y.; Nishio, M.; Mizobe, Y.; Hidai, M. *Organometallics* **1993**, *12*, 36. (h) Liaw, W.-F.; Kim, C.; Darensbourg, M. Y.; Rheingold, A. L. *J. Am. Chem. Soc.* **1989**, *111*, 3591. (i) Klein, D. P.; Kloster, G. M.; Bergman, R. G. *Ibid.* **1990**, *112*, 2022. (j) Carney, M. J.; Walsh, P. J.; Bergman, R. G. *Ibid.* **1990**, *112*, 6426. (k) Michelman, R. I.; Anderson, R. A.; Bergman, R. G. *Ibid.* **1991**, *113*, 5100. (l) Jones, W. D.; Dong, L. *Ibid.* **1991**, *113*, 559. (m) Dong, L.; Duckett, S. B.; Ohman, K. F.; Jones, W. D. *Ibid.* **1992**, *114*, 151. (n) Jones, W. D.; Chin, R. M. *Ibid.* **1992**, *114*, 9851. (o) Kajitani, A.; Sakurada, M.; Kakushi, D.; Suetsugu, T.; Akiyama, T.; Sugimori, A. *J. Chem. Soc., Chem. Commun.* **1990**, 19. (p) Sakurada, M.; Kajitani, M.; Hatano, H.; Matsudaira, Y.; Suetsugu, T.; Ono, S.; Akiyama, T.; Sugimori, A. *Organometallics* **1992**, *11*, 2337. (q) Ohtani, M.; Ookoshi, S.; Kajitani, M.; Akiyama, T.; Sugimori, A.; Yamauchi, S.; Ohba, Y.; Iwaizumi, M. *Inorg. Chem.* **1992**, *31*, 3873. (r) Cruz-Garritz, D.; Garcia-Alejandre, J.; Torrens, H.; Alvarez, C.; Toscano, R. A.; Poilblanc, R.; Thorez, A. *Transition Met. Chem.* **1991**, *16*, 130. (s) Osakada, K.; Matsumoto, K.; Yamamoto, T.; Yamamoto, A. *Organometallics* **1985**, *4*, 857. (t) Osakada, K.; Maeda, M.; Nakamura, Y.; Yamamoto, T.; Yamamoto, A. *J. Chem. Soc., Chem. Commun.* **1986**, 442. (u) Osakada, K.; Chiba, T.; Nakamura, Y.; Yamamoto, T.; Yamamoto, A. *Ibid.* **1986**, 1589. (v) Kim, Y.-J.; Osakada, K.; Sugita, K.; Yamamoto, T.; Yamamoto, A. *Organometallics* **1988**, *7*, 2182. (w) Osakada, K.; Chiba, T.; Yamamoto, T.; Yamamoto, A. *Ibid.* **1989**, *8*, 2602. (x) Osakada, K.; Ozawa, Y.; Yamamoto, A. *J. Chem. Soc., Dalton Trans.* **1991**, 759.

(2) (a) Okamura, H.; Miura, M.; Takei, H. *Tetrahedron Lett.* **1979**, 43. (b) Okamura, H.; Takei, H. *Ibid.* **1979**, 3425. (c) Murahashi, S.; Yamamura, M.; Yanagisawa, K.; Mita, N.; Kondo, K. *J. Org. Chem.* **1979**, *44*, 2408. (d) Kosugi, M.; Shimizu, T.; Migita, T. *Chem. Lett.* **1978**, 13. (e) Migita, T.; Shimizu, T.; Asami, Y.; Shiobara, J.; Kato, Y.; Kosugi, M. *Bull. Chem. Soc. Jpn.* **1980**, *53*, 1385. (f) Hutchins, R. O.; Learn, K. *J. Org. Chem.* **1982**, *47*, 4380. (g) Wenkert, E.; Leftin, M. H.; Michelotti, E. L. *J. Chem. Soc., Chem. Commun.* **1984**, 617. (h) Wenkert, E.; Hanna, J. M., Jr.; Leftin, M. H.; Michelotti, E. L.; Potts, K. T.; Usifer, D. *J. Org. Chem.* **1985**, *50*, 1125. (i) Tiecco, M.; Testaferri, L.; Tingoli, M.; Chianelli, D.; Wenkert, E. *Tetrahedron Lett.* **1982**, *23*, 4629. (j) Ni, Z.-J.; Mei, N. W.; Shi, X.; Wang, M. C.; Tzeng, Y.-L.; Luh, T.-Y. *J. Org. Chem.* **1991**, *56*, 4035. (k) Wong, K.-T.; Luh, T.-Y. *J. Am. Chem. Soc.* **1992**, *114*, 7308. (l) Osakada, K.; Yamamoto, T.; Yamamoto, A. *Tetrahedron Lett.* **1987**, *27*, 6321.

(3) (a) Osakada, K.; Hataya, K.; Yamamoto, T. *Inorg. Chem.* **1993**, *32*, 2360. (b) Osakada, K.; Hataya, K.; Tanaka, M.; Nakamura, Y.; Yamamoto, T. *J. Chem. Soc., Chem. Commun.* **1993**, 576.

0276-7333/93/2312-3358$04.00/0

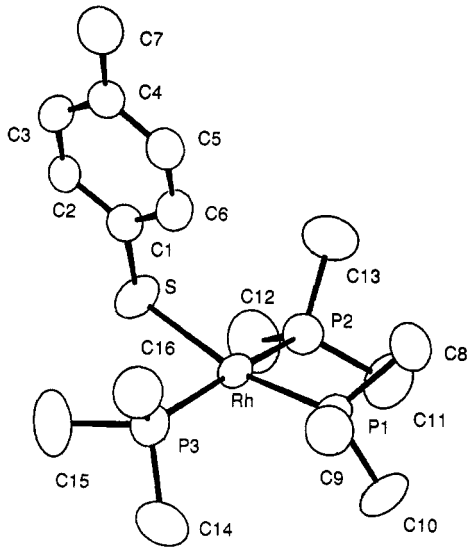

Figure 1. Molecular structure of $Rh(SC_6H_4$-*p*-$Me)(PMe_3)_3$ (**1**) showing ellipsoidal plotting at the 50% level.

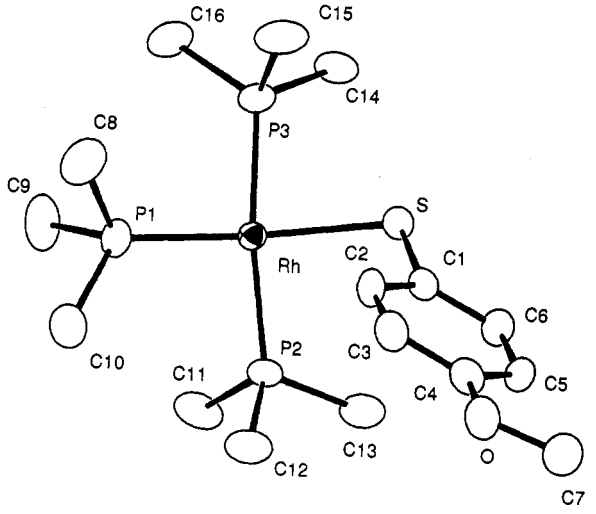

Figure 2. Molecular structure of $Rh(SC_6H_4$-*p*-$OMe)(PMe_3)_3$ (**2**) showing ellipsoidal plotting at the 50% level.

Table I. Selected Bond Distances (Å) and Angles (deg) of Complexes $Rh(SPh)(PMe_3)_3$, 1, and 2[a]

	$Rh(SPh)(PMe_3)_3$[b]	1	2
Rh–S	2.428(2)	2.412(2)	2.393(2)
Rh–P1	2.229(3)	2.229(2)	2.234(2)
Rh–P2	2.292(2)	2.293(3)	2.284(2)
Rh–P3		2.298(3)	2.305(2)
S–C1	1.748(9)	1.765(6)	1.775(6)
S–Rh–P1	162.99(9)	165.74(6)	164.94(7)
S–Rh–P2	85.72(5)	84.32(7)	90.61(7)
S–Rh–P3		90.04(7)	83.85(6)
P1–Rh–P2	96.36(5)	94.32(7)	95.09(7)
P1–Rh–P3		94.58(7)	94.46(8)
P2–Rh–P3	162.3(1)	164.66(7)	162.44(7)
Rh–S–C1	105.0(3)	103.9(2)	104.6(2)

[a] P1 is the phosphorus atom trans to the thiolato ligand, while P2 and P3 are cis to the thiolato ligand. [b] Data were taken from ref 3a. P3 is crystallographically equivalent to P2 due to the presence of a crystallographic mirror plane including Rh, P1, and S.

$Rh(SPh)(PMe_3)_3$ (2.428(2) Å) > **1** (2.412(2) Å) > **2** (2.393(2) Å), while the S–C bond distances increase in the order $Rh(SPh)(PMe_3)_3$ (1.748(9) Å) < **1** (1.765(6) Å) < **2** (1.775(6) Å). The Rh–S–C angles of the above three thiolatorhodium complexes are almost similar to each other (105.0(3), 103.9(2), and 104.6(2)°, respectively). These angles are smaller than those of most transition metal complexes with a nonbridging benzenethiolato ligand already reported.[4]

Reactions of 1 and of 2 with Aromatic Thiol. Complexes **1** and **2** react with HSC_6H_4-*p*-Me and with HSC_6H_4-*p*-OMe, respectively, to undergo oxidative addition of the S–H bond of the thiols. Reaction of **2** with HSC_6H_4-*p*-OMe in hexane causes immediate deposition of *cis,mer*-$RhH(SC_6H_4$-*p*-$OMe)_2(PMe_3)_3$ (**5a**). Further

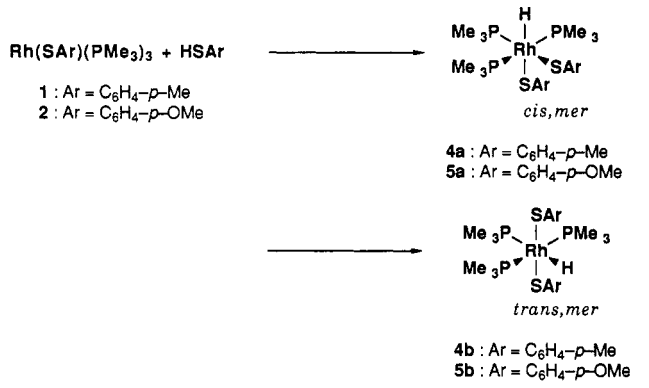

stirring the reaction mixture at room temperature causes gradual dissolution of **5a** to give the yellow to yellowish green solution from which *trans,mer*-$RhH(SC_6H_4$-*p*-$OMe)_2(PMe_3)_3$ (**5b**) is obtained. A similar reaction in C_6D_6 proceeds without deposition of the products. The ^1H NMR spectrum shows formation of **5a** and **5b** in a 1:2 ratio after reaction for 1 h, and **5a** in the mixture is turned into **5b** on further reaction at room temperature. Reaction of **1** with HSC_6H_4-*p*-Me in hexane also gives *cis,mer*-$RhH(SC_6H_4$-*p*-$Me)_2(PMe_3)_3$ (**4a**) and *trans,mer*-$RhH(SC_6H_4$-*p*-$Me)_2(PMe_3)_3$ (**4b**) as the initial and the final product. These results indicate that the cis,mer complexes are the kinetic products and the trans,mer complexes are the thermodynamic ones. The isomerization of **4a** to **4b** and of **5a** to **5b** is apparently irreversible since ^1H NMR spectra of the C_6D_6 solutions of **4b** and **5b** do not show any signal due to **4a** and **5a** on heating at 60–70 °C.

Facile isomerization of cis,mer to trans,mer Rh(III) complex was observed also in the already reported reaction of $Rh(SPh)(PMe_3)_3$ with HSPh.[3a] Previously, it was reported that oxidative addition of HCl to $RhCl(PEt_2Ph)_3$ initially gave *cis,mer*-$RhHCl_2(PEt_2Ph)_3$ which was turned into the thermodynamically more stable trans,mer isomer under the reaction conditions.[5,6] $IrBr(CO)(PR_3)_2$ was also reported to undergo oxidative addition of Ph_3SiH to give $Ir(Br)H(SiPh_3)(CO)(PR_3)_2$ with several structures as the kinetic and the thermodynamic products.[7] Several pathways seem to be possible as the mechanism of isomerization in the present study. A plausible path shown in Scheme I involves reductive elimination of thiol from the cis,mer complex to give $Rh(SAr)(PMe_3)_3$ which undergoes oxidative addition with the thiol, thus generating the thermodynamically more stable trans,mer complex. Another mechanism is also possible which involves initial dissociation of the thiolato ligand to give a cationic pentacoordinated intermediate which undergoes structural isomerization and ensuing coordination of the thiolato ligand to

(4) Ashby, M. T. *Comments Inorg. Chem.* **1990**, *10*, 297.
(5) Sacco, A.; Ugo, R.; Moles, A. *J. Chem. Soc. A* **1966**, 1670.
(6) Henderson, R. A. *J. Chem. Soc., Dalton Trans.* **1985**, 2067.
(7) Kunin, A. J.; Farid, R.; Johnson, C. E.; Eisenberg, R. *J. Am. Chem. Soc.* **1985**, *107*, 5315.

Table II. Reactions of *cis,mer*- and *trans,mer*-RhH(SPh)$_2$(PMe$_3$)$_3$ with HSC$_6$H$_4$-*p*-OMe and of 5a and 5b with HSPh[a]

starting materials		product[b]	
complex (amt, mmol)	thiol (amt, mmol)	SPh:SC$_6$H$_4$-*p*-OMe[c]	yield, %[d]
cis,mer-RhH(SPh)$_2$(PMe$_3$)$_3$ (0.15)	HSC$_6$H$_4$-*p*-OMe (0.63)	21:79 (32:68)	53
trans,mer-RhH(SPh)$_2$(PMe$_3$)$_3$ (0.21)	HSC$_6$H$_4$-*p*-OMe (0.83)	54:46 (34:66)	60
5a (0.13)	HSPh (0.97)	88:12 (79:21)	57
5b (0.17)	HSPh (0.97)	79:21 (74:26)	51

[a] Reactions were carried out at room temperature for 48 h. [b] *trans,mer*-RhH(SAr)$_2$(PMe$_3$)$_3$ isolated from the reaction mixture. [c] The ratio of the SPh and the SC$_6$H$_4$-*p*-OMe ligands in the product was determined from the ^{1}H NMR peak area ratio. In parentheses are the ratios of the Rh complex and the thiol used as the starting materials. [d] Yield based on the starting Rh complex. Calculated according to the formula RhH(SPh)$_x$(SC$_6$H$_4$-*p*-OMe)$_{2-x}$(PMe$_3$)$_3$ with the *x* value obtained as shown in *c*.

Scheme I

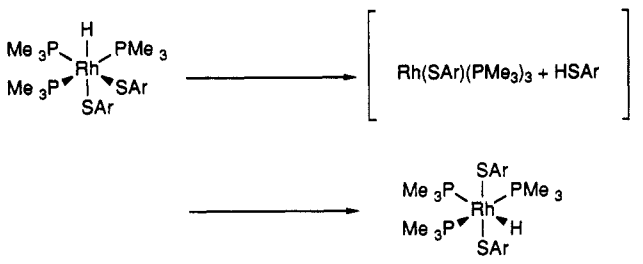

(Ar = Ph, C$_6$H$_4$-*p*-Me, C$_6$H$_4$-*p*-OMe)

give the trans,mer product. In order to compare the possible pathways, reactions of *cis,mer*- and *trans,mer*-RhH(SPh)$_2$(PMe$_3$)$_3$ with HSC$_6$H$_4$-*p*-OMe were carried out.

As shown in Table II the ^{1}H NMR spectrum of the Rh-containing product in the reaction of *cis,mer*-RhH(SPh)$_2$(PMe$_3$)$_3$ and HSC$_6$H$_4$-*p*-OMe (19:81) shows the signals due to the SPh and the SC$_6$H$_4$-*p*-OMe ligands bonded to the rhodium center. The peak area ratio between the OMe and the aryl hydrogens shows that the SPh and the SC$_6$H$_4$-*p*-OMe ligands are contained in a 21:79 ratio. The peak position and splitting pattern of the hydrido ligand agree with the *trans,mer*-bis(thiolato)hydridorhodium(III) complexes. These results suggest that the product contains a mixture of *trans,mer*-RhH(SPh)$_2$(PMe$_3$)$_3$, *trans,mer*-RhH(SPh)(SC$_6$H$_4$-*p*-OMe)(PMe$_3$)$_3$, and *trans,mer*-RhH(SC$_6$H$_4$-*p*-OMe)$_2$(PMe$_3$)$_3$, although they cannot be differentiated from each other by the ^{1}H NMR spectra. Reaction of *trans,mer*-RhH(SPh)$_2$(PMe$_3$)$_3$ and HSC$_6$H$_4$-*p*-OMe (20:80) gives a mixture of *trans,mer*-Rh(III) complexes containing the SPh and the SC$_6$H$_4$-*p*-OMe ligands in a 54:46 ratio.

In the former reaction starting from the *cis,mer*-Rh(III) complex, the ratio of the SPh and the SC$_6$H$_4$-*p*-OMe ligands in the product agrees with the molar ratio of *cis,mer*-RhH(SPh)$_2$(PMe$_3$)$_3$ and HSC$_6$H$_4$-*p*-OMe used in the reaction. On the other hand, the ratio among the thiolato ligands of the product in the latter reaction differs from the ratio among the thiolato groups contained in the starting materials.[8] As reported previously, reaction of *cis,mer*-RhH(SPh)$_2$(PMe$_3$)$_3$ with DSPh for 24 h at room temperature gave a mixture of *trans,mer*-RhH(SPh)$_2$(PMe$_3$)$_3$ and *trans,mer*-RhD(SPh)$_2$(PMe$_3$)$_3$ in a ratio which agreed with the H to D ratio contained in the hydrido ligand and the thiol group of the starting materials. On the other hand, H–D exchange of *trans,mer*-RhH(SPh)$_2$(PMe$_3$)$_3$ with DSPh, giving a mixture of *trans,mer*-RhH(SPh)$_2$(PMe$_3$)$_3$ and *trans,mer*-RhD(SPh)$_2$(PMe$_3$)$_3$, proceeded much slower and did not attain equilibrium in 24 h.[3a]

The results of the reactions of *cis,mer*- and *trans,mer*-RhH(SPh)$_2$(PMe$_3$)$_3$ with HSC$_6$H$_4$-*p*-OMe and with DSPh shown in the present and the previous papers indicate that the trans,mer complex undergoes a much slower ligand exchange reaction with ArSH than the cis,mer complex. The observation agrees with the isomerization path which involves reductive elimination and ensuing oxidative addition of the thiol (Scheme I)[9] rather than with that involving the dissociation of the thiolato ligand.[10]

The rate of the isomerization of *cis,mer*- to *trans,mer*-RhH(SPh)$_2$(PMe$_3$)$_3$ is influenced to a small extent by HSPh in the solution, as is observed from time dependent ^{31}P{^{1}H} NMR spectra of the reaction mixtures in the presence and in the absence of HSPh. The results also agree with the isomerization path in Scheme I involving reductive elimination of HSAr as the rate determining step.

Reactions of **5a** and **5b** with HSPh give mixtures of *trans,mer*-RhH(SAr)$_2$(PMe$_3$)$_3$ (Ar = Ph or C$_6$H$_4$-*p*-OMe). The ratios of the SPh and the SC$_6$H$_4$-*p*-OMe ligands in the products in both reactions are similar to the ratios in the starting materials. Much faster exchange of the SC$_6$H$_4$-*p*-OMe ligand in **5b** with the SPh group of HSPh than that of the SPh ligand in *trans,mer*-RhH(SPh)$_2$(PMe$_3$)$_3$ can be attributed to more facile reductive elimination of HSC$_6$H$_4$-*p*-OMe from **5b** than that of HSPh from *trans,mer*-RhH(SPh)$_2$(PMe$_3$)$_3$.

Experimental Section

All the manipulations of the complexes were carried out under nitrogen or argon using standard Schlenk techniques.

(8) The ratios of the SPh and the SC$_6$H$_4$-*p*-OMe ligands contained in the product are influenced not only by the ratio of the starting materials but also by the relative stability of the Rh–S bond between the SPh and the SC$_6$H$_4$-*p*-OMe ligand. The results obtained in the present study are not precise enough to discuss the relative stability of the Rh–S bond. However, the results indicate unambiguously the difference in the rate of the ligand substitution between the reaction of *cis,mer*-RhH(SPh)$_2$(PMe$_3$)$_3$ with HSC$_6$H$_4$-*p*-OMe and that of the trans,mer complex.

(9) The irreversible cis,mer to trans,mer isomerization through reductive elimination of HSAr and its reoxidative addition (Scheme I) seems to require that the structure of the intermediate "Rh(SAr)(PMe$_3$)$_3$" be different from that of the isolable Rh(SAr)(PMe$_3$)$_3$ (**1**, **2**) since the planar complex undergoes the oxidative addition with HSAr to give the cis,mer complex. The intermediate "Rh(SAr)(PMe$_3$)$_3$" is considered to be distorted from the square-planar coordination and is possibly a coordination with three P–Rh–S angles close to 90° as in the cis,mer complex and undergoes a very fast oxidative addition with HSAr before it is transformed into the planar complex. Although the pathway of oxidative addition of H$_2$ to RhCl(PPh$_3$)$_3$ was studied in detail by means of MO calculations, the plausible structure of the intermediate or the transition state has not been shown. See: Dedieu, A.; Strich, A. *Inorg. Chem.* **1979**, *18*, 2940.

(10) At present we cannot exclude the other mechanism involving S–H bond formation in the cis complex to give an HSAr coordinated intermediate that undergoes facile rotation of the Rh–HSAr bond followed by S–H bond cleavage to give the trans,mer complex. According to this mechanism, the incorporation of the deuterium and the thiolato group of thiol into the complex during the isomerization would be observed only when exchange of the coordinated HSAr with that in the solution occurs much faster than the above rotation of the Rh–HSAr bond.

$[Rh(PMe_3)_4]Cl$ and $RhCl(PMe_3)_3$ were prepared according to the literature method.[11] $NaSC_6H_4$-*p*-Me and $NaSC_6H_4$-*p*-OMe were prepared by reaction of the corresponding thiols with NaOEt in ethanol and stored under nitrogen atmosphere. IR spectra were recorded on a JASCO-IR810 spectrophotometer. NMR spectra (^1H, ^{13}C, and ^{31}P) were recorded on JEOL FX-100 and GX-500 spectrometers. Elemental analyses were carried out on a Yanagimoto Type MT-2 CHN autocorder and Yazawa Halogen and Sulfur Analyzer.

Preparation of $Rh(SC_6H_4$-*p*-$Me)(PMe_3)_3$ (1) and $Rh(SC_6H_4$-*p*-$OMe)(PMe_3)_3$ (2). To a Schlenk flask containing $[Rh(PMe_3)_4]Cl$ (390 mg, 0.88 mmol) and $NaSC_6H_4$-*p*-Me (180 mg, 1.2 mmol) was added hexane (40 mL) at room temperature. After the orange reaction mixture was stirred for 18 h, the deposited white solid was removed to give a red solution. The solvent was reduced to ca. 15 mL to give an orange solid. Gently heating the reaction mixture (ca. 50 °C) to dissolve the solid followed by cooling the mixture gave $Rh(SC_6H_4$-*p*-$Me)(PMe_3)_3$ (1) as orange blocks (190 mg, 42%). ^1H NMR (100 MHz, in C_6D_6): δ 1.17 (bs, 27H, $P(CH_3)_3$), 2.18 (s, 3H, C_6H_4-*p*-CH_3), 6.48 and 8.15 (d, 4H, C_6H_4, J(HH) = 8 Hz). $^{31}P\{^1H\}$ NMR (40 MHz in C_6D_6, ppm from external H_3PO_4): −13.6 (bs). Anal. Calcd for $C_{16}H_{34}P_3RhS$: C, 42.3; H, 7.5; S, 7.1. Found: C, 42.0; H, 7.6; S, 6.5.

$Rh(SC_6H_4$-*p*-$OMe)(PMe_3)_3$ (2) was prepared analogously (38%). ^1H NMR (100 MHz, in C_6D_6): δ 1.17 (bs, 27H, $P(CH_3)_3$), 3.73 (s, 3H, C_6H_4-*p*-OCH_3), 6.76 and 8.12 (d, 4H, C_6H_4, J(HH) = 9 Hz). $^{31}P\{^1H\}$ NMR (40 MHz in C_6D_6, ppm from external H_3PO_4): −13.9 (bs). IR (KBr): 1233 cm^{-1} (ν(C−O)). Anal. Calcd for $C_{16}H_{34}OP_3RhS$: C, 40.9; H, 7.3; S, 6.8. Found: C, 40.4; H, 7.4; S, 6.6.

Preparation of $Rh(SC_6H_4$-*p*-$Me)(O_2)(PMe_3)_3$ (3). To a Schlenk flask containing a hexane (15 mL) solution of complex 1 (0.23 mmol) was introduced air at room temperature. An orange solid was deposited immediately from the red solution. After the reaction mixture was stirred under air for 0.5 h, the orange solid was filtered out and washed with a small amount of hexane to give **3** (84 mg, 75%). ^1H NMR (100 MHz, in C_6D_6): δ 1.29 (apparent triplet by virtual coupling,[12] 18H, $P(CH_3)_3$), 1.51 (d, 9H, $P(CH_3)_3$, J = 9 Hz), 2.18 (s, 3H, C_6H_4-*p*-CH_3), 6.81 and 7.34 (d, C_6H_4, J = 6 Hz). Anal. Calcd for $C_{16}H_{34}O_2P_3RhS$: C, 39.5; H, 7.0; S, 6.6. Found: C, 39.3; H, 7.4; S, 6.6.

Preparation of *cis,mer*-$RhH(SC_6H_4$-*p*-$Me)_2(PMe_3)_3$ (4a) and *cis,mer*-$RhH(SC_6H_4$-*p*-$OMe)_2(PMe_3)_3$ (5a). To a Schlenk flask containing a hexane (20 mL) solution of 1 (0.49 mmol) was added a hexane (3 mL) solution of HSC_6H_4-*p*-Me (61 mg, 0.49 mmol). After stirring for 5 min, the solvent was reduced to ca. 3 mL to cause deposition of a yellow solid which was filtered out and washed with a small amount of hexane to give *cis,mer*-$RhH(SC_6H_4$-*p*-$Me)_2(PMe_3)_3$ (4a) (190 mg, 67%). ^1H NMR (100 MHz, in C_6D_6): δ −13.53 (ddt, 1H, Rh*H*, J(RhH) = J(PH) = 17 Hz), 0.99 (d, 9H, $P(CH_3)_3$, J(PH) = 8 Hz), 1.23 (bs, 18H, $P(CH_3)_3$), 2.17 (s, 6H, C_6H_4-*p*-CH_3), 6.83–7.20 and 7.94–8.04 (m, C_6H_4, 8H). IR (KBr): 2010 cm^{-1} (ν(Rh−H)). Anal. Calcd for $C_{23}H_{42}P_3RhS_2$: C, 47.8; H, 7.3; S, 11.1. Found: C, 47.8; H, 7.4; S, 10.9.

cis,mer-$RhH(SC_6H_4$-*p*-$OMe)_2(PMe_3)_3$ (5a) was prepared analogously (80%). ^1H NMR (100 MHz, in C_6D_6): δ −13.57 (ddt, 1H, Rh*H*, J(RhH) = J(PH) = 17 Hz), 1.09 (d, 9H, $P(CH_3)_3$, J(PH) = 7 Hz), 1.33 (bs, 18H, $P(CH_3)_3$), 3.37 (s, 6H, C_6H_4-*p*-OCH_3), 6.80–7.18 and 7.80–8.13 (m, C_6H_4, 8H). IR (KBr): 2010 cm^{-1} (ν(Rh−H)), 1230 cm^{-1} (ν(C−O)). Anal. Calcd for $C_{23}H_{42}O_2P_3RhS_2$: C, 45.3; H, 6.9; S, 10.5. Found: C, 47.3; H, 7.1; S, 10.6.[13]

Preparation of *trans,mer*-$RhH(SC_6H_4$-*p*-$Me)_2(PMe_3)_3$ (4b) and *trans,mer*-$RhH(SC_6H_4$-*p*-$OMe)_2(PMe_3)_3$ (5b). To a Schlenk flask containing a hexane (20 mL) solution of 1 (0.49 mmol) was added a hexane (3 mL) solution of HSC_6H_4-*p*-Me (61 mg, 0.49 mmol). A yellow solid was deposited soon. The reaction mixture was stirred at room temperature to cause dissolution of the solid. After further stirring of the reaction mixture for 48 h, the solvent was reduced to ca. 10 mL. Cooling the resulting yellow solution at −20 °C gave *trans,mer*-$RhH(SC_6H_4$-*p*-$Me)_2(PMe_3)_3$ (4b) as yellow crystals (230 mg, 81%). ^1H NMR (100 MHz, in C_6D_6): δ −8.54 (ddt, 1H, Rh*H*, J(RhH) = 11 Hz, J(PH) = 184 and 18 Hz), 1.06 (d, 9H, $P(CH_3)_3$, J(PH) = 7 Hz), 1.29 (apparent triplet due to virtual coupling, 18H, $P(CH_3)_3$), 2.15 (s, 6H, C_6H_4-*p*-CH_3), 6.95 and 8.04 (d, C_6H_4, 8 H, J = 8 Hz). $^{31}P\{^1H\}$ NMR (40 MHz in C_6D_6, ppm from external 85% H_3PO_4): −11.2 (dd, J(RhP) = 98 Hz, J(PP) = 27 Hz), −29.3 (dt, J(RhP) = 82 Hz, J(PP) = 27 Hz). IR (KBr): 2026 cm^{-1} (ν(Rh−H)). Anal. Calcd for $C_{23}H_{42}P_3RhS_2$: C, 47.8; H, 7.3; S, 11.1. Found: C, 47.4; H, 7.5; S, 10.8.

trans,mer-$RhH(SC_6H_4$-*p*-$OMe)_2(PMe_3)_3$ (5b) was prepared analogously (78%). ^1H NMR (100 MHz, in C_6D_6): δ −8.68 (ddt, 1H, Rh*H*, J(RhH) = 12 Hz, J(PH) = 185 and 18 Hz), 1.08 (d, 9H, $P(CH_3)_3$, J(PH) = 7 Hz), 1.32 (apparent triplet due to virtual coupling, 18H, $P(CH_3)_3$), 3.35 (s, 6H, C_6H_4-*p*-OCH_3), 7.02 and 8.12 (d, C_6H_4, 8 H, J = 8 Hz). $^{31}P\{^1H\}$ NMR (40 MHz in C_6D_6, ppm from external 85% H_3PO_4): −11.4 ppm (dd, J(RhP) = 96 Hz, J(PP) = 27 Hz), −29.3 ppm (dt, J(RhP) = 81 Hz, J(PP) = 27 Hz). IR (KBr): 2000 cm^{-1} (ν(Rh−H)), 1232 cm^{-1} (ν(C−O)). Anal. Calcd for $C_{23}H_{42}O_2P_3RhS_2$: C, 45.3; H, 6.9; S, 10.5. Found: C, 44.6; H, 6.8; S, 10.2.

Reactions of *cis,mer*- and *trans,mer*-$RhH(SPh)_2(PMe_3)_3$ with HSC_6H_4-*p*-OMe and of 5a and 5b with HSPh. To a Schlenk flask containing *cis,mer*-$RhH(SPh)_2(PMe_3)_3$ (85 mg, 0.15 mmol) was added a toluene (5 mL) solution of HSC_6H_4-*p*-OMe (0.63 mmol). After the resulting solution was stirred for 48 h at room temperature, the solvent was reduced to ca. 0.5 mL under high vacuum. Addition of hexane (5 mL) to the reaction mixture followed by evacuation of the solvent (to ca. 0.5 mL) and readdition of hexane (5 mL) caused deposition of a yellow solid (43 mg). The ^1H NMR spectrum of the product in C_6D_6 showed that the ratio of the SPh and SC_6H_4-*p*-OMe ligands in the product is 21:79.

Reaction of *trans,mer*-$RhH(SPh)_2(PMe_3)_3$ with HSC_6H_4-*p*-OMe as well as reactions of **5a** and of **5b** with HSPh were carried out analogously.

^{31}P NMR Monitoring of Isomerization of *cis,mer*- to *trans,mer*-$RhH(SPh)_2(PMe_3)_3$ in the Presence and in the Absence of HSPh. To an NMR tube containing a C_6D_6 (0.4 mL) solution of *cis,mer*-$RhH(SPh)_2(PMe_3)_3$ (43 mg, 0.080 mmol) was added HSPh (88 mg, 0.80 mmol) at −60 °C. The $^{31}P\{^1H\}$ NMR spectrum of the mixture was measured periodically on keeping the mixture at 25 °C. The peak integration shows ratios of the cis,mer and the trans,mer complexes of 71:29 (after the reaction for 0.5 h at 25 °C), 50:50 (after 1 h), 25:75 (after 2 h), and 15:85 (after 3 h), respectively. Similar measurement of the reaction mixture without added HSPh shows ratios of 80:20 (after 0.5 h), 58:42 (after 1 h), 34:66 (after 2 h), and 22:78 (after 3 h).

X-ray Structural Characterization. A Rigaku AFC-5R diffractometer was used for X-ray crystal structure determination using graphite monochromated Mo Kα radiation (λ = 0.710 69 Å). Table III summarizes the crystal data and details in the structure refinement of 1 and 2. Tables IV and V show atomic coordinates of the complexes. Cell constants were determined and refined on the basis of setting angles of 25 reflections with 2θ = 25–35°. Systematic absences of the intensity data for 1 and 2 indicated unambiguously the space groups $P2_1/n$ (No. 14) and $P2_12_12_1$ (No. 19), respectively. Periodic measurement of the standard peaks of 2 indicated deterioration of the peak intensity to 92% during the data collection, while 1 did not show a decrease in the standard peak intensity. The intensity measurements were corrected for Lorentz and polarization effects, and an empirical absorption correction (ψ scan) was applied after positions of all the non-hydrogen atoms were refined anisotropically. Structure calculations were carried out using the program

(11) Price, R. T.; Anderson, R. A.; Muetterties, E. L. *J. Organomet. Chem.* **1989**, *376*, 407.

(12) Pregosin, P. S.; Kunz, W. *^{31}P and ^{13}C NMR of Transition Metal Phosphine Complexes*; Springer-Verlag: Heidelberg, 1979; pp 65–68.

(13) Examination of elemental analysis of **5a** does not give satisfactory results, possibly due to contamination of the solvent used during recrystallization of the complex.

Table III. Crystallographic Data and Details of Structure Refinement of Complexes 1 and 2

complex	1	2
chemical formula	$C_{16}H_{34}P_3SRh$	$C_{16}H_{32}OP_3SRh$
fw	454.35	470.35
cryst syst	monoclinic	orthorhombic
space group	$P2_1/n$ (No. 14)	$P2_12_12_1$ (No. 19)
a, Å	12.879(5)	11.811(2)
b, Å	12.677(4)	20.546(4)
c, Å	13.506(2)	9.522(2)
β, deg	94.06(2)	
V, Å^3	2199	2311
Z	4	4
μ, cm^{-1}	10.65	10.19
$F(000)$	944	976
ρ_{calcd}, g cm^{-3}	1.372	1.352
cryst size, mm	0.3 × 0.3 × 0.4	0.4 × 0.4 × 0.6
2θ range, deg	5.0–55.0	5.0–50.0
scan rate, deg min^{-1}	4	8
no. of unique reflns	4850	2347
no. of used reflns ($F_o \geq 3\sigma(F_o)$)	2479	1762
$R(F_o)^a$	0.039	0.027
$R_w(F_o)^a$	0.046	0.030
weighting scheme	$[\{\sigma(F_o)\}^2]^{-1}$	$[\{\sigma(F_o)\}^2]^{-1}$

^{a} $R = \sum||F_o| - |F_c||/\sum|F_o|$, $R_w = [\sum w(|F_o| - |F_c|)^2/\sum w|F_o|^2]^{1/2}$.

Table IV. Atomic Coordinates and Equivalent Isotropic Temperature Factors of 1

atom	x	y	z	B_{eq}, Å^2
Rh	0.36980(3)	0.24930(4)	0.23057(3)	3.17
S	0.2012(1)	0.1691(1)	0.1968(1)	4.81
P1	0.5042(1)	0.3599(1)	0.2508(1)	3.63
P2	0.3842(1)	0.2289(1)	0.0634(1)	4.31
P3	0.3583(1)	0.2214(1)	0.3975(1)	4.17
C1	0.1128(5)	0.2711(5)	0.2201(4)	3.5
C2	0.0066(4)	0.2490(5)	0.2205(4)	3.6
C3	−0.0649(4)	0.3277(5)	0.2325(5)	3.8
C4	−0.0353(5)	0.4317(5)	0.2451(5)	4.0
C5	0.0695(5)	0.4538(5)	0.2456(5)	4.3
C6	0.1437(5)	0.3757(5)	0.2357(5)	4.3
C7	−0.1121(6)	0.5194(6)	0.2537(6)	6.0
C8	0.4979(6)	0.4693(5)	0.1630(6)	5.7
C9	0.5243(6)	0.4406(6)	0.3624(5)	5.8
C10	0.6375(5)	0.3146(6)	0.2408(7)	6.4
C11	0.5095(6)	0.2367(7)	0.0077(6)	6.8
C12	0.3464(7)	0.0994(7)	0.0162(6)	7.3
C13	0.3031(6)	0.3145(7)	−0.0168(6)	7.2
C14	0.4782(6)	0.1747(7)	0.4616(5)	6.2
C15	0.2714(7)	0.1162(7)	0.4319(6)	7.2
C16	0.3157(6)	0.3266(7)	0.4772(5)	6.0

system TEXSAN[14] on a DEC Micro VAXII computer. Atomic scattering factors were taken from the literature.[15] Positions of the non-hydrogen atoms of the complexes were determined by direct methods and the subsequent Fourier technique. The hydrogen atoms with isotropic temperature factors were located at idealized positions and were included in the structure calculation without refinement of their parameters. Final R and R_w values of **1** and **2** are in Table III. The chiral conformation of **2** was determined by comparison of the R factors between two stereoisomeric conformations.

Table V. Atomic Coordinates and Equivalent Isotropic Temperature Factors of 2

atom	x	y	z	B_{eq}, Å^2
Rh	0.02522(3)	0.12578(2)	0.25208(6)	2.98
S	0.1374(1)	0.22051(8)	0.2072(2)	3.88
P1	−0.0466(2)	0.03371(9)	0.3393(2)	4.31
P2	0.0841(2)	0.08025(9)	0.0458(2)	3.86
P3	−0.0640(2)	0.19192(9)	0.4133(2)	4.21
O	0.6112(4)	0.1234(2)	0.1848(6)	5.4
C1	0.2783(5)	0.1910(3)	0.1950(7)	3.5
C2	0.3170(5)	0.1410(3)	0.2815(7)	4.2
C3	0.4270(6)	0.1199(3)	0.2775(7)	4.5
C4	0.5027(5)	0.1479(3)	0.1806(9)	4.2
C5	0.4661(5)	0.1965(3)	0.0934(6)	3.6
C6	0.3547(6)	0.2182(3)	0.1030(7)	4.0
C7	0.6931(6)	0.1554(4)	0.1029(9)	5.8
C8	−0.0246(9)	0.0273(5)	0.5309(9)	6.9
C9	−0.1956(6)	0.0125(4)	0.3181(12)	7.7
C10	0.0155(7)	−0.0450(3)	0.2907(10)	6.6
C11	−0.0318(8)	0.0403(5)	−0.0474(10)	6.6
C12	0.1961(6)	0.0199(4)	0.0311(10)	6.3
C13	0.1314(8)	0.1347(4)	−0.0915(7)	7.0
C14	0.0202(7)	0.2125(5)	0.5661(8)	6.8
C15	−0.1016(7)	0.2719(3)	0.3427(9)	6.2
C16	−0.1996(7)	0.1713(4)	0.4956(10)	6.8

Acknowledgment. We are grateful to Drs. Masako Tanaka and Yoshiyuki Nakamura in our laboratory for their help with the crystallography and NMR measurement, respectively. This work was financially supported by Grants-in-Aid for Scientific Research from the Ministry of Education, Science and Culture, Japan (03855182 and 04805084).

Supplementary Material Available: Tables of anisotropic thermal factors, fractional coordinates of hydrogen atoms, and all bond distances and angles (14 pages). Ordering information is given on any current masthead page.

OM930177K

(14) Sweptson, P. N. *TEXSAN software*; Molecular Structure Corp.: College Station, TX, 1986.
(15) *International Tables for X-ray Crystallography*; Kynoch: Birmingham, England, 1974; Vol. IV.